**Supporting Information**

# Microfluidic device for rapid digestion of tissues into cellular suspensions

Xiaolong Qiu,[#a] Trisha M. Westerhof,[#c] Amrith A. Karunaratne,[a] Erik M. Werner,[a] Pedram P. Pourfard,[a] Edward L. Nelson,[cde] Elliot E. Hui,[a] and Jered B. Haun*[abe]

[a] Department of Biomedical Engineering, University of California, Irvine, Irvine, CA 92697, USA.

[b] Department of Chemical Engineering and Materials Science, University of California, Irvine, Irvine, CA 92697, USA.

[c] Department of Medicine, Division of Hematology/Oncology, School of Medicine, University of California, Irvine, Irvine, CA 92697, USA.

[d] Department of Molecular Biology and Biochemistry, University of California, Irvine, Irvine, CA 92697, USA.

[e] Chao Family Comprehensive Cancer Center, University of California, Irvine, Irvine, CA 92697, USA.

[#] These authors contributed equally to this work.

**Table of Contents**

Figure S1 Image processing algorithm to monitor tissue digestion.

Figure S2 Mouse kidney and liver tissue imaging and CyQUANT data.

Figure S3 Flow cytometry gating scheme

Figure S4 Mouse kidney and liver cell viability data

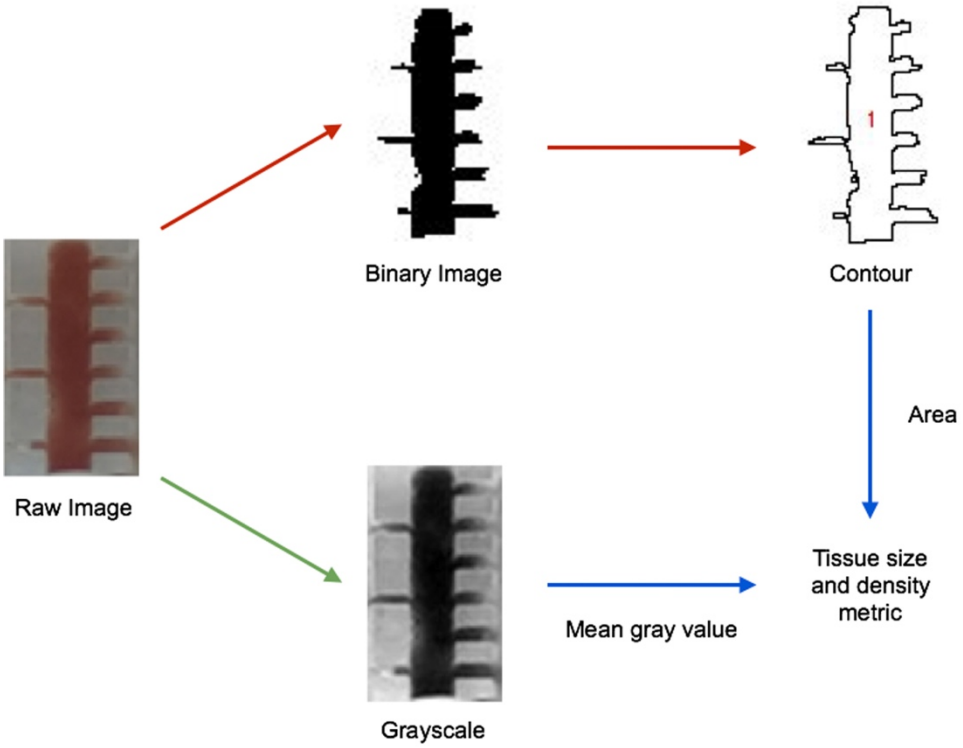


**Figure S1. Image processing algorithm to monitor tissue digestion.** Images were analyzed for tissue size and density to quantify changes during digestion within the device. First, raw images were separately converted to binary (red arrow) and grayscale (green arrow) images to outline the contour and quantify mean gray value, respectively. The area within the tissue contour was then calculated, and multiplied by mean gray value to obtain a single metric accounting for tissue size and density.

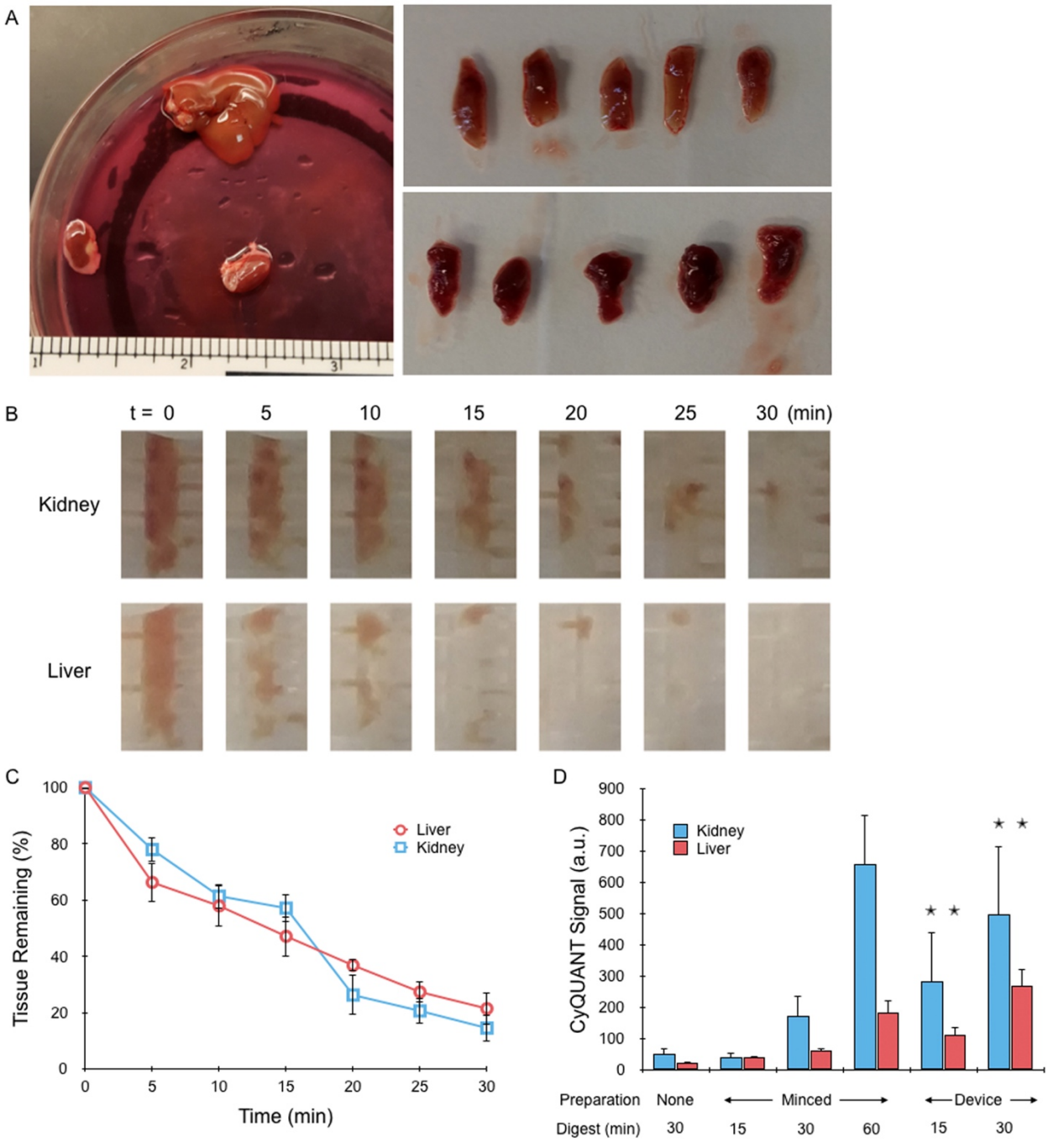
A
B
t = 0
5
10
15
20
25
30 (min)
Kidney
Liver
C
Tissue Remaining (%)
Time (min)
Liver
Kidney
D
CyQUANT Signal (a.u.)
Kidney
Liver
Preparation
None
Minced
Device
Digest (min)
30
15
30
60
15
30

**Figure S2. Mouse kidney and liver tissue imaging and CyQUANT data.** (A) Mouse liver (top) and kidneys (bottom) were freshly harvested and cut into 1 cm long x 1 mm diameter pieces and placed within the device sample chamber. (B) Time-lapse images of tissue digestion for the device containing 3 hydro-mince channels. Tissue size and density both decreased over time as digestion progressed. (C) Tissue loss was quantified from images based on mean gray value and overall tissue area, with liver and kidney samples demonstrating similar trends. (D) CyQUANT assay was used to directly quantify cell suspensions obtained by digestion only, scalpel mincing and digestion, or device treatment lasting for a total of 15, 30, or 60 min. CyQUANT signal increased with treatment time, and was higher overall for kidney samples. Signals from device treated samples were consistently higher than minced controls, similar to gDNA and cell counting results presented in Fig. 3 of the main text. Error bars represent standard errors from at least three independent experiments. * indicates $p < 0.05$ relative to minced control at the same digestion time.

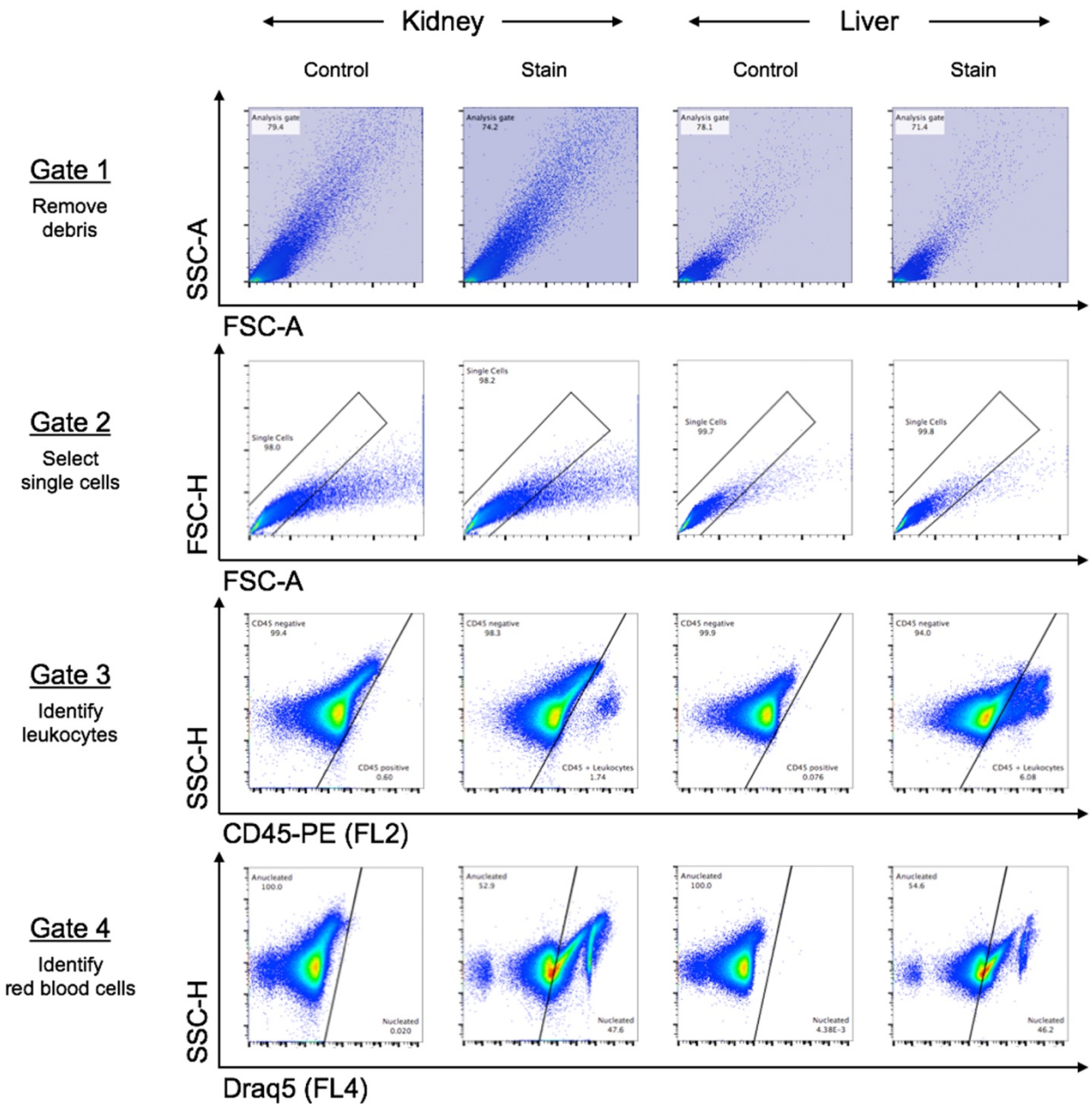
Kidney
Liver
Control
Stain
Control
Stain
Gate 1
Remove debris
SSC-A
FSC-A
Analysis gate 79.4
Analysis gate 74.2
Analysis gate 78.1
Analysis gate 71.4
Gate 2
Select single cells
FSC-H
FSC-A
Single Cells 98.0
Single Cells 98.2
Single Cells 99.7
Single Cells 99.8
Gate 3
Identify leukocytes
SSC-H
CD45-PE (FL2)
CD45 negative 99.4
CD45 positive 0.60
CD45 negative 98.3
CD45 + Leukocytes 1.74
CD45 negative 99.9
CD45 positive 0.076
CD45 negative 94.0
CD45 + Leukocytes 6.08
Gate 4
Identify red blood cells
SSC-H
Draq5 (FL4)
Anucleated 100.0
Nucleated 0.020
Anucleated 52.9
Nucleated 47.6
Anucleated 100.0
Nucleated 4.38E-3
Anucleated 54.6
Nucleated 46.2

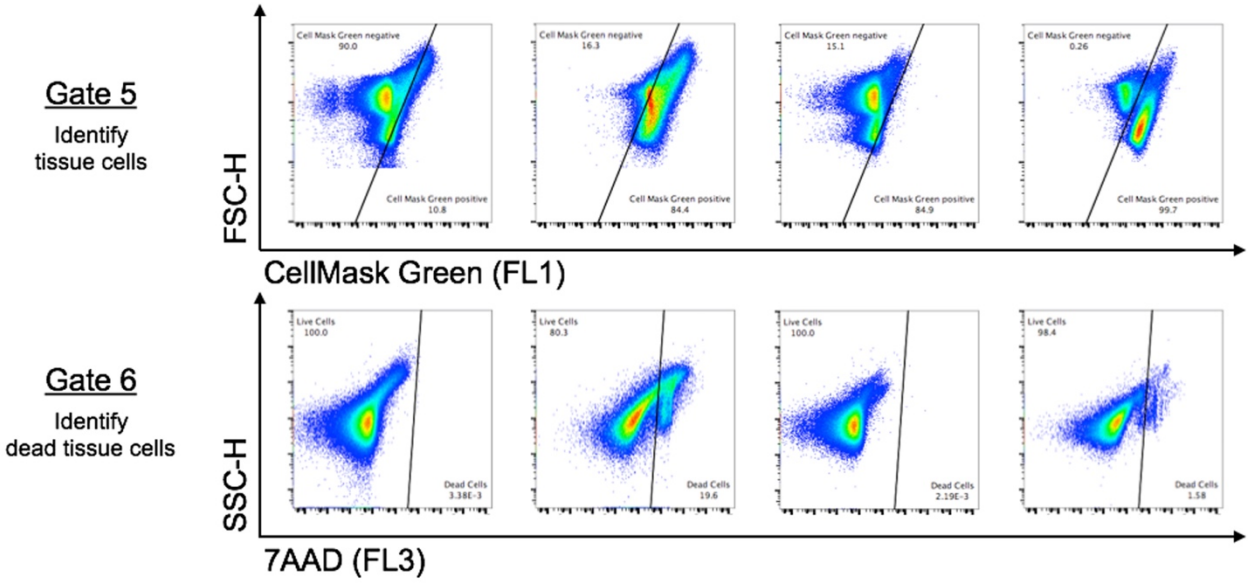


**Figure S3. Flow cytometry gating scheme.** Cell suspensions obtained from digested mouse liver and kidney samples were stained with the four-probe panel listed in Table 1 and analyzed using flow cytometry. Controls were treated only with an isotype matched (IgG2b), PE-conjugated antibody. Acquired data was assessed using a sequential gating scheme. First, an FSC-A vs. SSC-A gate (Gate 1) was used to exclude debris near the origin. Gate 2 was based on FSC-A vs. FSC-H, and was used to select single cells. Gate 3 distinguished CD45+ leukocytes based on CD45-PE signal in FL2-A vs. SSC-H plots. The CD45- cell subset was further divided into anucleate RBCs and nucleated tissue cell subsets based on signal from the DRAQ5 nuclear stain in FL4-A vs. SSC-H plots. The cellularity of nucleated tissue cells of interest was validated based on signal of the cell membrane dye CellMask Green in FL1-A vs. FSC-H plots. Finally, live and dead tissue cells were discriminated based on 7-AAD signal in FL3-A vs. SSC-H plots. All gates were established using the minced control that was digested for 60 min. Heat treated cells were used as a positive control to confirm appropriate 7-AAD signal for dead cells.

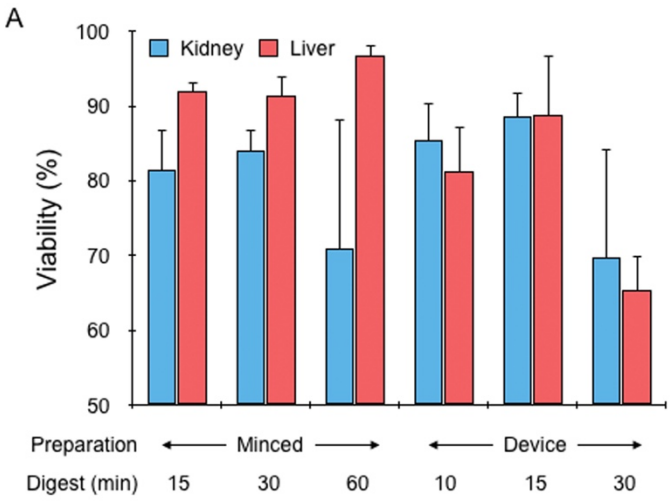


**Figure S4. Mouse kidney and liver cell viability data.** (A) Cell viability was similar for device treated conditions relative to minced counterparts, demonstrating minimal effect of device treatment. Error bars represent standard errors from at least three independent experiments.